

**Decay of  $^{201-203}\text{Ra}$  and  $^{200-202}\text{Fr}$** 

Z. Kalaninová,<sup>1,\*</sup> S. Antalic,<sup>1</sup> A. N. Andreyev,<sup>2,3</sup> F. P. Heßberger,<sup>4,5</sup> D. Ackermann,<sup>4</sup> B. Andel,<sup>1</sup> L. Bianco,<sup>6</sup> S. Hofmann,<sup>4</sup> M. Huyse,<sup>7</sup> B. Kindler,<sup>4</sup> B. Lommel,<sup>4</sup> R. Mann,<sup>4</sup> R. D. Page,<sup>6</sup> P. J. Sapple,<sup>6</sup> J. Thomson,<sup>6</sup> P. Van Duppen,<sup>7</sup> and M. Venhart<sup>8,1</sup>

<sup>1</sup>*Department of Nuclear Physics and Biophysics, Comenius University, 84248 Bratislava, Slovakia*

<sup>2</sup>*Department of Physics, University of York, York YO10 5DD, United Kingdom*

<sup>3</sup>*Advanced Science Research Center, Japan Atomic Energy Agency, Tokai-mura, Ibaraki 319-1195, Japan*

<sup>4</sup>*GSI Helmholtzzentrum für Schwerionenforschung GmbH, 64291 Darmstadt, Germany*

<sup>5</sup>*Helmholtz Institut Mainz, 55099 Mainz, Germany*

<sup>6</sup>*Department of Physics, Oliver Lodge Laboratory, University of Liverpool, Liverpool L69 7ZE, United Kingdom*

<sup>7</sup>*KU Leuven, Instituut voor Kern- en Stralingsfysica, 3001 Leuven, Belgium*

<sup>8</sup>*Institute of Physics, Slovak Academy of Sciences, 84511 Bratislava, Slovakia*

(Received 21 March 2014; published 12 May 2014)

Decay properties of the neutron-deficient nuclides  $^{201-203}\text{Ra}$  and  $^{200-202}\text{Fr}$  were investigated using  $\alpha$ - and  $\gamma$ -decay spectroscopy. The nuclei were produced in fusion-evaporation reactions of  $^{56}\text{Fe}$  projectiles with enriched  $^{147}\text{Sm}$  and  $^{149}\text{Sm}$  targets at the velocity filter SHIP at GSI in Darmstadt (Germany). The  $\alpha$  decay from the  $(3/2^-)$  state in  $^{201}\text{Ra}$  was identified with an energy  $E_\alpha = 7842(12)$  keV and half-life  $T_{1/2} = 8^{+40}_{-4}$  ms. Ambiguous decay properties for  $^{202}\text{Ra}$  from previous measurements were clarified by remeasuring with significantly improved precision, resulting in values of  $E_\alpha = 7722(7)$  keV and  $T_{1/2} = 3.8^{+1.3}_{-0.8}$  ms. New short-lived isomeric states were identified in  $^{200}\text{Fr}$  and  $^{201}\text{Fr}$  with half-lives of  $0.6^{+0.5}_{-0.2}$   $\mu\text{s}$  and  $0.7^{+0.5}_{-0.2}$   $\mu\text{s}$ , respectively. A tentative spin and parity of  $13/2^+$  were assigned to the latter. One event attributed to  $\beta$ -delayed fission of  $^{200}\text{Fr}$  was observed.

DOI: [10.1103/PhysRevC.89.054312](https://doi.org/10.1103/PhysRevC.89.054312)

PACS number(s): 23.60.+e, 23.20.Lv, 21.10.Tg, 27.80.+w

**I. INTRODUCTION**

The region of neutron-deficient nuclei above lead ( $Z = 82$ ) provides possibilities to investigate several interesting phenomena, such as the coexistence of different shapes within a single nucleus (e.g., Ref. [1] and references therein) and  $\beta$ -delayed fission. The latter enables fission to be studied at low excitation energies in nuclei whose ground states do not undergo spontaneous fission (e.g., Refs. [2,3] and references therein).

In this region of the chart of nuclides, the energies of a number of excited single-particle levels within a given isotopic chain decrease when going towards lighter isotopes. As a consequence, in the lightest nuclides several single-particle levels that may correspond to different deformations are located very close to the Fermi surface. It has been proposed that the ground state for most of the neutron-deficient odd- $A$  bismuth ( $Z = 83$ ) and astatine ( $Z = 85$ ) isotopes is related to a  $\pi h_{9/2}$  spherical configuration (e.g., Refs. [4,5]). It has also been suggested that this ground state coexists with states related to a proton excitation to the  $i_{13/2}$  orbital or a proton hole in the  $s_{1/2}$  orbital, giving rise to an oblate deformation (e.g., Ref. [6]).

Recent experiments aimed at a detailed investigation of the light odd- $A$  francium isotopes ( $Z = 87$ ) indicate the existence of coexisting shapes in these nuclides as well. An intruder  $1/2^+$  state was identified in  $^{201,203}\text{Fr}$  using  $\alpha$ -decay spectroscopy [7]. Isomeric  $1/2^+$  and  $13/2^+$  states were observed in  $^{203}\text{Fr}$  [8] and  $^{205}\text{Fr}$  [9] using prompt in-beam  $\gamma$ -ray, delayed  $\gamma$ -ray, and electron spectroscopy, in addition to  $\alpha$ -decay

studies. Both the  $1/2^+$  and  $13/2^+$  states are assumed to possess oblate deformations and to coexist with the spherical  $9/2^-$  ground state [7–9]. (We note that for simplicity we do not put tentative spins and parities in parentheses in the text, but we keep them in the figures.)

For the even-even nuclides, coexisting structures were also seen in light polonium ( $Z = 84$ ) (e.g., Ref. [10]) and radon ( $Z = 86$ ) (e.g., Ref. [11]) isotopes. This effect can be also expected in radium ( $Z = 88$ ) isotopes, but there is presently not much experimental information available.

In this work we present results for the neutron-deficient radium and francium nuclides  $^{201-203}\text{Ra}$  and  $^{200-202}\text{Fr}$  investigated by  $\alpha$ - and  $\gamma$ -decay spectroscopy. We report on the identification of new  $\alpha$ - and  $\gamma$ -decaying states in these nuclides and present significantly improved  $\alpha$ -decay data for  $^{202}\text{Ra}$ . The identification of a small  $\beta$ -delayed fission branch is reported for  $^{200}\text{Fr}$ .

**II. EXPERIMENT**

Neutron-deficient radium and francium nuclides were produced at GSI in Darmstadt using fusion-evaporation reactions of a  $^{56}\text{Fe}$  ion beam with isotopically enriched  $^{147}\text{Sm}$  and  $^{149}\text{Sm}$  targets. The beam with an average intensity  $\sim 600$  pA ( $1$  pA =  $6.242 \times 10^9$  particles/s) was provided by the Universal Linear Accelerator (UNILAC). Several beam energies in the range of (236–275) MeV were used. Targets with a thickness of  $\sim 370$   $\mu\text{g}/\text{cm}^2$  were prepared from  $^{147}\text{SmF}_3$  and  $^{149}\text{SmF}_3$  materials with isotopic enrichment of 96.4% and 96.9%, respectively. They were evaporated on a 40- $\mu\text{g}/\text{cm}^2$  carbon backing and covered with a 10- $\mu\text{g}/\text{cm}^2$  carbon layer to avoid sputtering of the target material and to increase the emissivity of the target. Targets were mounted on a wheel

\*zdenka.kalaninova@fmph.uniba.sk

rotating synchronously to the beam macro structure (5 ms long pulses at 50 Hz repetition frequency).

Products of fusion-evaporation reactions were separated from unwanted particles (projectiles, scattered target nuclei, transfer products) by the velocity filter SHIP (separator for heavy ion reaction products) [12] and were transmitted with an efficiency of 40% to the focal-plane detector system. After separation, evaporation residues (ERs) were implanted into a 300- $\mu\text{m}$  thick 16-strip position-sensitive silicon detector (PSSD). The energy resolution of the PSSD for  $\alpha$  particles was  $\sim 25$  keV (FWHM). The detection efficiency of 7-MeV  $\alpha$  particles with full-energy release in the PSSD was 56%. For energy calibration of the PSSD we used  $\alpha$  decays of nuclei produced in the reaction  $^{56}\text{Fe} + ^{141}\text{Pr}$  studied before the irradiation of samarium targets: 6311(5) keV ( $^{191}\text{Bi}$ ), 6609(5) keV ( $^{195}\text{Po}^g$ ), 6699(5) keV ( $^{195}\text{Po}^m$ ), 6843(3) keV ( $^{194}\text{Po}$ ) [13]. Alpha particles escaping from the PSSD in the backward direction were registered by a system of six silicon strip detectors (denoted as “BOX” in the following text) with a geometric efficiency 80% of  $2\pi$  [14]. The energy resolution of the PSSD + BOX system was  $\sim 70$  keV (FWHM) for the registration of escaping  $\alpha$  particles.

Three time-of-flight (TOF) detectors [15] were installed in front of the PSSD. The (anti)coincidence signals between the TOF detectors and the PSSD enabled implantations of ions to be distinguished from decays. Distinction between complete-fusion reaction products and other implanted particles was achieved by measuring their time of flight and kinetic energy.

For the detection of  $\gamma$  rays a germanium clover detector composed of four crystals was placed behind the PSSD in close geometry. Gamma rays were recorded either as “individual” events or in coincidence with signals from the PSSD within a time window of 5  $\mu\text{s}$ . The energy resolution of the germanium detector was 1.4 keV (FWHM) at  $E_\gamma \approx 80$  keV. The detection efficiency for  $\sim 80$ -keV  $\gamma$  rays was  $\sim 10\%$  [16].

Nuclides were identified using time and position correlations of subsequent signals (see Ref. [17] for more details on the correlation method). The position difference between an ER implantation and its  $\alpha$  decay (ER- $\alpha 1$  correlations) and between two subsequent  $\alpha$  decays ( $\alpha 1$ - $\alpha 2$  correlations) was required to be within  $\pm 0.5$  mm.

### III. RESULTS AND DISCUSSIONS

#### A. Isotope $^{202}\text{Ra}$

##### 1. Experimental results

Prior to this study, only two  $\alpha$ -decay events with significantly different values for the  $\alpha$ -decay energies and life-times were reported for  $^{202}\text{Ra}$ . Both events were registered in experiments at the gas-filled recoil separator RITU at the Department of Physics of the University of Jyväskylä (JYFL) in Finland. One event was produced in the reaction  $^{36}\text{Ar} + ^{170}\text{Yb}$  at a beam energy of 201 MeV yielding  $E_\alpha = 7860(60)$  keV,  $T_{1/2} = 0.7^{+3.3}_{-0.3}$  ms [18]. The  $\alpha$  particle tentatively assigned to the decay of  $^{202}\text{Ra}$  was followed by two escaped  $\alpha$  particles. Another triple- $\alpha$  correlation chain was observed in the reaction  $^{63}\text{Cu} + ^{141}\text{Pr}$  at a beam energy of (278–288) MeV yielding  $E_\alpha = 7740(20)$  keV,  $T_{1/2} = 16^{+30}_{-7}$  ms [7]. In this case the

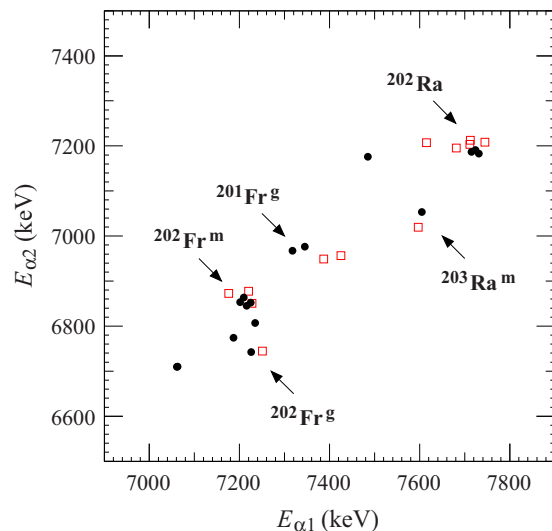


FIG. 1. (Color online) Correlation parent-daughter  $\alpha 1$ - $\alpha 2$  energy spectrum measured in the PSSD + BOX system in the reaction  $^{56}\text{Fe} + ^{149}\text{Sm}$  at  $E_{\text{beam}} = 244$  and 256 MeV. Correlation search times were  $\Delta t(\text{ER}-\alpha 1) < 50$  ms and  $\Delta t(\alpha 1-\alpha 2) < 300$  ms. Full circles represent events with both  $\alpha 1$  and  $\alpha 2$  particles fully stopped in the PSSD, while open squares represent cases where the  $\alpha 1$  or  $\alpha 2$  particle (or both) were registered with the PSSD + BOX system.

daughter  $\alpha$  particle escaped while the granddaughter decay was registered with full energy.

We collected decay data for  $^{202}\text{Ra}$  at several beam energies in the range of (244–275) MeV (in front of the  $^{149}\text{Sm}$  target). The corresponding excitation energy of the compound nuclei was in the range of (30–53) MeV for production at 2/3 of the target thickness, which is the most probable location for the formation of the evaporation residues. Time windows of  $\Delta t(\text{ER}-\alpha 1) < 50$  ms and  $\Delta t(\alpha 1-\alpha 2) < 300$  ms were used to search for  $^{202}\text{Ra}$ . Sixteen ER- $\alpha 1$ - $\alpha 2$  decay chains were registered with parent decay characteristics of  $E_{\alpha 1} = 7722(7)$  keV,  $T_{1/2} = 3.8^{+1.3}_{-0.8}$  ms and daughter decay characteristics of  $E_{\alpha 2} = 7198(6)$  keV,  $T_{1/2} = 38^{+13}_{-8}$  ms (see Fig. 1 and Table I). For all the ER- $\alpha 1$ - $\alpha 2$  chains we found the correlated granddaughter  $\alpha 3$  decay with  $E_{\alpha 3} = 6846(7)$  keV and  $T_{1/2} = 340^{+110}_{-70}$  ms. Daughter  $\alpha 2$ - and granddaughter  $\alpha 3$ -decay properties correspond to  $^{198}\text{Rn}$  (reference values:  $E_\alpha = 7205(5)$  keV,  $T_{1/2} = 64(2)$  ms [19]) and  $^{194}\text{Po}$  (reference

TABLE I. The  $\alpha$ -decay properties of  $^{201,202}\text{Ra}$ .

Isotope	$I^\pi$	$E_\alpha$ (keV)	$T_{1/2}$ (ms)	$\delta_\alpha^2$ (keV)	Ref.
$^{201}\text{Ra}$	$3/2^-$	7842(12)	$8^{+40}_{-4}$	$43^{+204}_{-20}$	this work
	$13/2^+$	7905(20)	$1.6^{+7.7}_{-0.7}$	$140^{+680}_{-70}$ <sup>a</sup>	[7]
$^{202}\text{Ra}$	$0^+$	7722(7)	$3.8^{+1.3}_{-0.8}$	$210^{+70}_{-50}$	this work
	$0^+$	7740(20)	$16^{+30}_{-7}$	$44^{+83}_{-20}$ <sup>a</sup>	[7]
	$0^+$	7860(60)	$0.7^{+3.3}_{-0.3}$	$430^{+2020}_{-260}$ <sup>a</sup>	[18]

<sup>a</sup>Values of  $\delta_\alpha^2$  were calculated according to the Rasmussen prescription [21] using input values ( $E_\alpha$  and  $T_{1/2}$ ) from cited references.

values:  $E_\alpha = 6842(6)$  keV,  $T_{1/2} = 392(4)$  ms [20]), respectively. Thus, we assigned the parent  $\alpha 1$  activity to  $^{202}\text{Ra}$ . The maximum cross section for the production of  $^{202}\text{Ra}$ , 0.2(1) nb, was measured at  $E_{\text{beam}} = 244$  MeV.

From the number of registered  $\alpha$  decays of  $^{198}\text{Rn}$  and  $^{194}\text{Po}$  we obtained an  $\alpha$ -decay branching ratio of more than 88% for  $^{194}\text{Po}$ . This value agrees with the value of 93(7)% from Ref. [20]. One of the 16 detected events of  $^{202}\text{Ra}$  was registered in the irradiation of the  $^{147}\text{Sm}$  target. However, in this case we suppose that  $^{202}\text{Ra}$  was produced in the reaction with  $^{149}\text{Sm}$ , which was a 0.53% admixture in the  $^{147}\text{Sm}$  target, as the cross section for the reaction  $^{149}\text{Sm}(^{56}\text{Fe}, 3n)^{202}\text{Ra}$  is considerably higher than that for  $^{147}\text{Sm}(^{56}\text{Fe}, 1n)^{202}\text{Ra}$ .

## 2. Discussion

The  $\alpha$ -decay properties for the two  $^{202}\text{Ra}$  events registered in previous experiments resulted in reduced  $\alpha$ -decay widths of  $430^{+2020}_{-260}$  [18] and  $44^{+83}_{-20}$  keV [7]. One of them indicated a tendency of lowering  $\delta_\alpha^2$  at decreasing neutron number in radium isotopes, while the other indicated an increasing trend. Both trends have been observed for even-even isotopes of neighboring elements [see Fig. 2(a)] and their interpretation is discussed in Ref. [22]. We deduced the reduced  $\alpha$ -decay width using the Rasmussen prescription [21] assuming  $\Delta L = 0$  and obtained  $\delta_\alpha^2 = 210^{+70}_{-50}$  keV for the 7722-keV  $\alpha$  decay of  $^{202}\text{Ra}$ , confirming unambiguously the trend of increasing  $\delta_\alpha^2$ . Recent results also show the tendency of increasing  $\delta_\alpha^2$  in neighboring thorium [23] and radon [24,25]

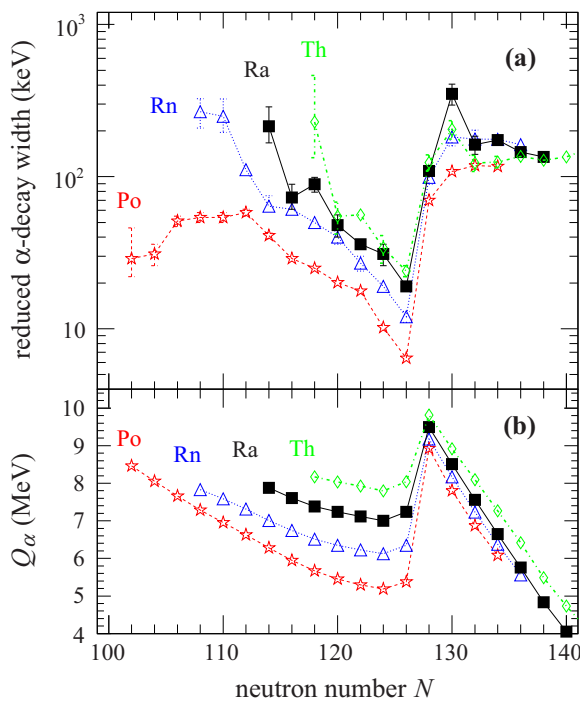


FIG. 2. (Color online) (a) Systematics of reduced  $\alpha$ -decay widths for even-even isotopes of elements from polonium ( $Z = 84$ ) to thorium ( $Z = 90$ ) in the vicinity of the shell closure  $N = 126$ . (b) Systematics of  $Q_\alpha$  values for the nuclides from (a). Literature values are taken from Refs. [22,23,26].

isotopes. The improved value of  $Q_\alpha$  [7.878(7) MeV] for  $^{202}\text{Ra}$  obtained from our measurement follows the trend of  $Q_\alpha$  values for radium isotopes [see Fig. 2(b)].

## B. Isotope $^{201}\text{Ra}$

### 1. Experimental results

Prior to our measurement, only one ER- $\alpha 1$ - $\alpha 2$ - $\alpha 3$ (escaped) decay chain originating from  $^{201}\text{Ra}$  was observed in an experiment performed at RITU at JYFL [7]. The event was produced in the reaction  $^{63}\text{Cu} + ^{141}\text{Pr}$  at  $E_{\text{beam}} = (278\text{--}288)$  MeV yielding  $E_{\alpha 1} = 7905(20)$  keV and  $T_{1/2} = 1.6^{+7.7}_{-0.7}$  ms. The  $\alpha 2$  and  $\alpha 3$  decays were attributed to originate from the  $13/2^+$  states in  $^{197}\text{Rn}$  and  $^{193}\text{Po}$ , respectively. A spin and parity of  $13/2^+$  was also assigned to the corresponding state in  $^{201}\text{Ra}$ , because the  $\alpha 1$  decay was considered to be unhindered.

We registered one ER- $\alpha 1$ - $\alpha 2$ (escaped)- $\alpha 3$  correlation chain with  $E_{\alpha 1} = 7842(12)$  keV and  $\Delta t(\text{ER}-\alpha 1) = 12.0$  ms in the reaction with the  $^{147}\text{Sm}$  target at a beam energy of 249 MeV, corresponding to an excitation energy of  $E^* = 27$  MeV in the compound nucleus (see Fig. 3). The parent  $\alpha 1$  decay was followed by the daughter  $\alpha 2$  decay after 51 ms. The  $\alpha 2$  particle escaped from the PSSD, depositing only part of its energy (4191 keV). The  $\alpha 3$  decay with  $E_{\alpha 3} = 6947(12)$  keV was detected with full energy in the PSSD 644 ms after the  $\alpha 2$  decay.

We assign the  $\alpha 3$  decay to the known decay of the  $3/2^-$  state in  $^{193}\text{Po}$  (with reference values  $E_\alpha = 6949(5)$  keV,  $T_{1/2} = 450(40)$  ms [20]). The measured time difference between  $\alpha 1$  and  $\alpha 2$  decays,  $\Delta t(\alpha 1-\alpha 2) = 51$  ms, agrees with the known half-life of the  $3/2^-$  state in  $^{197}\text{Rn}$  (reference value is  $65^{+25}_{-14}$  ms [27]). Based on the properties of the  $\alpha 2$  and  $\alpha 3$  decay, we attribute the parent 7842(12)-keV  $\alpha 1$  decay with  $T_{1/2} = 8^{+40}_{-4}$  ms to  $^{201}\text{Ra}$  (see Table I). The probability for the detection of such a triple- $\alpha$  correlation chain randomly,

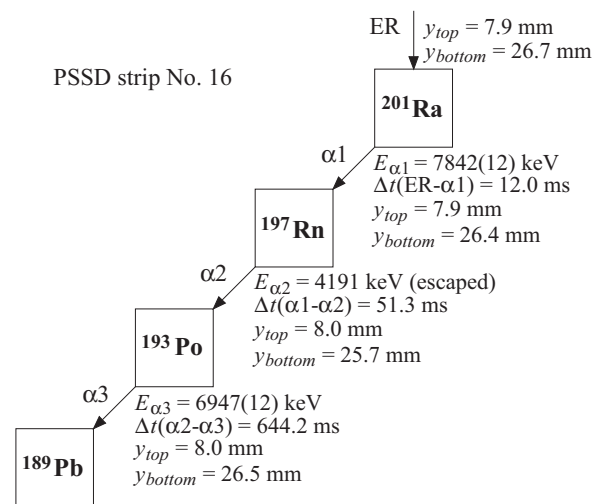


FIG. 3. Observed  $\alpha$ -decay chain attributed to  $^{201}\text{Ra}$ . Measured energies in the PSSD, time differences between subsequent signals and, positions obtained from the top ( $y_{\text{top}}$ ) and bottom ( $y_{\text{bottom}}$ ) of the strip are shown. The  $\alpha 1$  and  $\alpha 3$  particles were fully stopped in the PSSD, while the  $\alpha 2$  particle escaped.

calculated using the method from Ref. [28], is  $10^{-8}$ . The production cross section for  $^{201}\text{Ra}$  was evaluated as  $40_{-30}^{+80}$  pb at  $E_{\text{beam}} = 249$  MeV.

In the reaction  $^{56}\text{Fe} + ^{147}\text{Sm}$  we also searched for the decay of  $^{200}\text{Ra}$  applying ER- $\alpha 1(^{200}\text{Ra})$ - $\alpha 2(^{196}\text{Rn})$  and ER-proton( $^{200}\text{Ra})$ - $\alpha(^{199}\text{Fr})$  correlation search. However, no appropriate chain was found. The estimated upper limit for the production cross section of  $^{200}\text{Ra}$  is 30 pb at the beam energy of 263 MeV, corresponding to the expected maximum of the  $^{200}\text{Ra}$  excitation function.

## 2. Discussion

The reduced width of the observed 7842(12)-keV  $\alpha$  decay from  $^{201}\text{Ra}$  is  $43_{-20}^{+204}$  keV. The reduced  $\alpha$ -decay widths for heavier even- $A$  radium isotopes are  $210_{-50}^{+70}$  ( $^{202}\text{Ra}$  [this work]) and  $73_{-12}^{+16}$  keV ( $^{204}\text{Ra}$  [18]). For the heavier odd- $A$  radium isotopes  $^{203}\text{Ra}$  and  $^{205}\text{Ra}$ , reduced  $\alpha$ -decay widths of around 60 keV are known for both the  $3/2^-$  and  $13/2^+$   $\alpha$ -decaying states [7,18]. Based on these values we assume no change in spin and parity between the states connected by the 7842(12)-keV  $\alpha 1$  transition from  $^{201}\text{Ra}$ . As we assigned the observed  $\alpha 2$  and  $\alpha 3$  decays to the  $3/2^-$  state in daughter nuclei  $^{197}\text{Rn}$  and  $^{193}\text{Po}$ , respectively, we conclude that the triple- $\alpha$  correlation chain originates from the  $3/2^-$  state in  $^{201}\text{Ra}$  (see the proposed  $\alpha$ -decay scheme in Fig. 4). Alpha-decay energies of all isotopes in correlation chains detected in our work and Ref. [7] are different, which proves that a different state was populated in each study. The production cross section of the  $3/2^-$  state obtained from our data ( $40_{-30}^{+80}$  pb) is similar to the production cross section of the  $13/2^+$  state (25 pb [7]), reflecting the fact that only a single decay chain was measured for each state.

In most of the light radium and radon isotopes, the ground-state spin and parity is  $3/2^-$  (see Fig. 5). Nevertheless, the

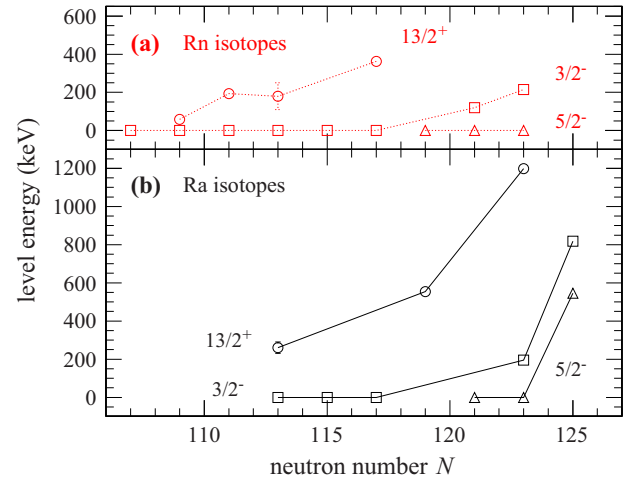


FIG. 5. (Color online) Single-particle level systematics for odd- $A$  (a) radon ( $Z = 86$ ) and (b) radium ( $Z = 88$ ) isotopes. Reference values are taken from Refs. [26,29].

energy of the  $13/2^+$  level decreases with lowering neutron number and we can expect both levels to lie close in energy in the most neutron-deficient region. The spin of the ground and isomeric state in  $^{189}\text{Pb}$  were determined unambiguously as  $3/2^-$  and  $13/2^-$ , respectively, by in-source laser spectroscopy at the on-line isotope mass separator ISOLDE at the European Organization for Nuclear Research (CERN) in Switzerland [29]. In that study the  $13/2^+$  isomeric level was located at 40(4) keV above the  $3/2^-$  ground state of  $^{189}\text{Pb}$ , which established the excitation energies of the  $13/2^+$  levels in  $^{193}\text{Po}$  and  $^{197}\text{Rn}$  to be 95(7) and 194(12) keV, respectively. On this basis we determine the excitation energy of the  $13/2^+$  level in  $^{201}\text{Ra}$  to be 260(30) keV.

## C. Isotope $^{203}\text{Ra}$

### 1. Experimental results and discussion

Seven decay chains assigned to  $^{203}\text{Ra}$  were observed in the fusion-evaporation reaction  $^{35}\text{Cl} + ^{175}\text{Lu}$  at  $E_{\text{beam}} = (191\text{--}208)$  MeV at RITU at JYFL [18]. Six decay chains were assigned to the  $13/2^+$  state and one decay chain was assigned to the  $3/2^-$  state. A subsequent measurement with improved precision was performed at RITU using the reactions  $^{65}\text{Cu} + ^{141}\text{Pr}$  at  $E_{\text{beam}} = (283\text{--}293)$  MeV and  $^{36}\text{Ar} + ^{170}\text{Yb}$  at  $E_{\text{beam}} = (180\text{--}185)$  MeV [7]. In this later study, two  $\alpha$ -decaying states were also observed. For both states altogether several tens of events were registered. Decay properties from both studies are in agreement (see Table II) except for the half-life of the  $3/2^-$  state, for which values of  $1.0_{-0.5}^{+5.0}$  ms [18] and  $31_{-9}^{+17}$  ms [7] were measured.

We observed nine decays of  $^{203}\text{Ra}$  in the reaction with the  $^{149}\text{Sm}$  target at beam energies in the range of (244–275) MeV, corresponding to an excitation energy range of  $E^* \approx (30\text{--}53)$  MeV for compound nuclei. Searching for these decays we used time windows  $\Delta t(\text{ER-}\alpha 1) < 300$  ms and  $\Delta t(\alpha 1\text{--}\alpha 2) < 3$  s. Two groups of decays were detected. The first one comprising five  $\alpha$ -decay chains had  $E_{\alpha 1} =$

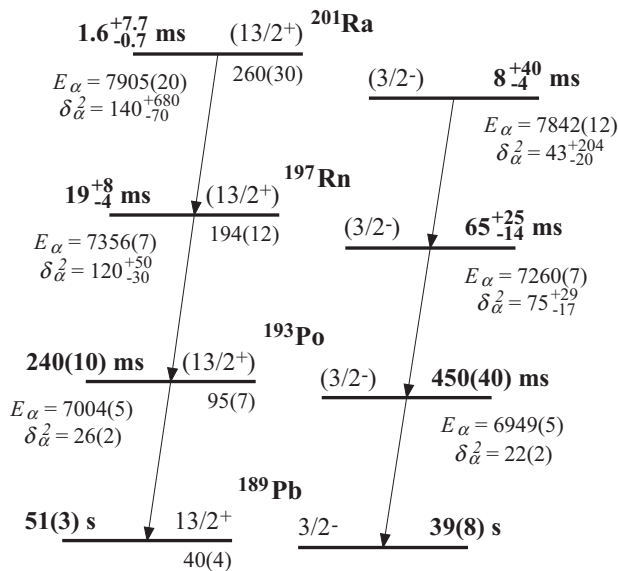


FIG. 4. Proposed  $\alpha$ -decay scheme for  $^{201}\text{Ra}$ . Values for the  $3/2^-$  ground state and the excitation energy of the  $13/2^+$  state in  $^{201}\text{Ra}$  are from this work; other values are from Refs. [7,20,27,29]. Alpha-decay energies, reduced widths, and energies of excited levels are in keV.

TABLE II. The  $\alpha$ -decay properties of  $^{203}\text{Ra}$  and its daughter  $^{199}\text{Rn}$ .

Isotope	$I^\pi$	$E_\alpha$ (keV)	$T_{1/2}$ (ms)	$\delta_\alpha^2$ (keV)	Ref.
$^{203}\text{Ra}$	$3/2^-$	7575(10)	$50^{+40}_{-15}$	$45^{+37}_{-14}$	this work
	$3/2^-$	7589(8)	$31^{+17}_{-9}$	$66^{+36a}_{-20}$	[7]
	$3/2^-$	7577(20)	$1.0^{+5.0}_{-0.5}$	$2200^{+11200a}_{-1200}$	[18]
	$13/2^+$	7607(8)	$37^{+37}_{-12}$	$48^{+48}_{-16}$	this work
	$13/2^+$	7612(8)	$24^{+6}_{-4}$	$72^{+18a}_{-13}$	[7]
	$13/2^+$	7615(20)	$33^{+22}_{-10}$	$51^{+35a}_{-17}$	[18]
$^{199}\text{Rn}$	$3/2^-$	6978(10)	$340^{+280}_{-110}$	$120^{+100}_{-40}$	this work
	$3/2^-$	6989(6)	$1100^{+900}_{-400}$	$34^{+28a}_{-12}$	[7]
	$3/2^-$	6995(10)	620(25)	$57(5)^a$	[30]
	$13/2^+$	7050(10)	$120^{+120}_{-40}$	$190^{+190}_{-70}$	this work
	$13/2^+$	7060(6)	$260^{+80}_{-50}$	$82^{+26a}_{-16}$	[7]
	$13/2^+$	7059(10)	325(25)	$66(7)^a$	[30]

<sup>a</sup>See footnote in Table I.

7575(10) keV,  $T_{1/2} = 50^{+40}_{-15}$  ms for the parent  $\alpha 1$  decay and  $E_{\alpha 2} = 6978(10)$  keV,  $T_{1/2} = 340^{+280}_{-110}$  ms for the daughter  $\alpha 2$  decay. The other group of four  $\alpha$ -decay chains yielded  $E_{\alpha 1} = 7607(8)$  keV,  $T_{1/2} = 37^{+37}_{-12}$  ms for the parent  $\alpha 1$  decay and  $E_{\alpha 2} = 7050(10)$  keV,  $T_{1/2} = 120^{+120}_{-40}$  ms for the daughter  $\alpha 2$  decay. These two groups of ER- $\alpha 1$ - $\alpha 2$  chains were attributed to the decays of the  $3/2^-$  and  $13/2^+$  states in  $^{203}\text{Ra}$ , respectively, based on previously measured reference values for  $^{203}\text{Ra}$  and its  $\alpha$ -decay daughter  $^{199}\text{Rn}$  (see Table II). Our results are in agreement with values in Ref. [7]. A maximum cross section of 0.2(1) nb was measured for the sum of both  $\alpha$ -decaying states in  $^{203}\text{Ra}$  at  $E_{\text{beam}} = 244$  MeV.

The ratio of decays from the  $13/2^+$  and  $3/2^-$  state from our data is 0.8(5). In contrast to this, more decays were seen from the  $13/2^+$  state than from the  $3/2^-$  state in both previous studies with reported ratio of  $\sim 6$  [18] and  $\sim 3$  [7]. However, the statistics in all experiments were low (9 events in our work, 7 events in Ref. [18] and  $\sim 30$  events in Ref. [7]).

Spins and parities of  $3/2^-$  and  $13/2^+$  were previously assigned to the two  $\alpha$ -decaying states in  $^{203}\text{Ra}$  [18]. We confirm these assignments based on reduced  $\alpha$ -decay widths obtained from our data (see Table II) and the assumed unhindered character of the  $\alpha$  decays. We note that energy difference between the ground  $3/2^-$  and isomeric  $13/2^+$  states is not known, either for  $^{203}\text{Ra}$  or for its  $\alpha$ -decay daughters.

#### D. Isotope $^{200}\text{Fr}$

##### 1. Experimental results

The detection of the isotope  $^{200}\text{Fr}$  was reported for the first time at the gas-filled recoil separator GARIS at the Institute of Physical and Chemical Research (RIKEN) in Japan [31]. Six ER- $\alpha 1$ - $\alpha 2$  decay chains were observed. The same number of six events was also obtained at RITU at JYFL [32]. Half-life values from these two studies were  $570^{+270}_{-140}$  ms [31] and  $19^{+13}_{-6}$  ms [32]. Later, in an experiment carried out at the ISOLDE facility at CERN, significantly higher statistics for

 TABLE III. The  $\alpha$ -decay properties of  $^{200}\text{Fr}$  and its daughter  $^{196}\text{At}$ .

Isotope	$E_\alpha$ (keV)	$I_\alpha$ (%)	$T_{1/2}$ (ms)	$\delta_\alpha^2$ (keV)	Ref.
$^{200}\text{Fr}$	7470(5)		46(4)	48(5)	this work
	7468(15)		$37^{+30}_{-12}$	44(8)	[34]
	7473(12)		49(4)	$44(5)^a$	[33]
	7468(9)		$19^{+13}_{-6}$	$120^{+80a}_{-40}$	[32]
	7500(30)		$570^{+270}_{-140}$	$3.1^{+1.6a}_{-1.0}$	[31]
	$^{196}\text{At}$	7045(5)	96(2)	350(90)	29(8)
6732(8)		4(2)		17(9)	this work
7048(12)			$350^{+290}_{-110}$	27(2)	[34]
7055(12)			389(54)	$25(4)^a$	[33]
7048(5)			388(7)	$27(1)^a$	[35]
7065(30)			253(9)	$36(9)^a$	[36]
7044(7)			$390^{+270}_{-120}$	$28^{+19a}_{-9}$	[32]
7053(30)			$320^{+220}_{-90}$	$31^{+23a}_{-12}$	[31]

<sup>a</sup>See footnote in Table I.

$^{200}\text{Fr}$  were collected and a half-life of 49(4) ms was measured [33] (see Table III).

In our experiment the isotope  $^{200}\text{Fr}$  was produced in the complete-fusion reaction  $^{56}\text{Fe} + ^{147}\text{Sm}$ . Data were collected at beam energies of 260 and 263 MeV resulting in  $E^* \approx 35$  and 37 MeV of the compound nuclei, respectively. Searching for correlated  $\alpha$  decays of  $^{200}\text{Fr}$  and its daughter  $^{196}\text{At}$  we used time windows  $\Delta t(\text{ER-}\alpha 1) < 0.3$  s and  $\Delta t(\alpha 1-\alpha 2) < 2$  s. A two-dimensional plot of correlated parent-daughter ( $\alpha 1$ - $\alpha 2$ ) events is shown in Fig. 6. In this spectrum we marked as ‘‘A’’ and ‘‘B’’ two groups attributed to the decay of  $^{200}\text{Fr}$ . Parent  $\alpha 1$ -decay properties for both groups [ $E_{\alpha 1} = 7470(5)$  keV,  $T_{1/2} = 46(4)$  ms for group A and  $E_{\alpha 1} = 7463(12)$  keV,  $T_{1/2} =$

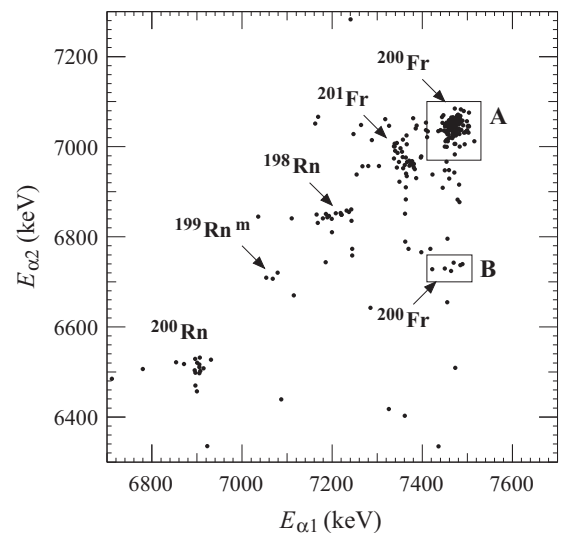


FIG. 6. Parent-daughter  $\alpha 1$ - $\alpha 2$  correlation energy spectrum measured in the PSSD in anticoincidence with the TOF detectors in the reaction  $^{56}\text{Fe} + ^{147}\text{Sm}$  at  $E_{\text{beam}} = 260$  and 263 MeV. The correlation search times were  $\Delta t(\text{ER-}\alpha 1) < 0.3$  s and  $\Delta t(\alpha 1-\alpha 2) < 2$  s.

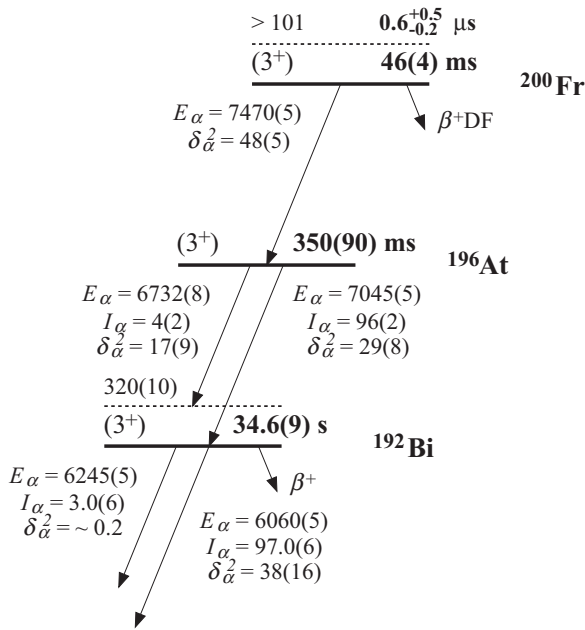


FIG. 7. Alpha-decay scheme for  $^{200}\text{Fr}$ . The values for  $^{200}\text{Fr}$  and  $^{196}\text{At}$  are from our data and for  $^{192}\text{Bi}$  are from Ref. [38]. Alpha-decay energies, reduced widths and energies of excited levels are in keV and relative intensities are in %.

$89_{-26}^{+61}$  ms for group B] correspond to the decay connecting ground states of  $^{200}\text{Fr}$  and  $^{196}\text{At}$ . The maximum cross section of 1.8(2) nb was measured for the production of  $^{200}\text{Fr}$  at  $E_{\text{beam}} = 263$  MeV.

The daughter  $\alpha$ 2-decay properties of group A [ $E_{\alpha 2} = 7045(5)$  keV,  $T_{1/2} = 340(90)$  ms] correspond to the transition connecting ground states of  $^{196}\text{At}$  and  $^{192}\text{Bi}$ . For the  $\alpha$ 2 decay of group B the measured energy and half-life are 6732(8) keV and  $670_{-200}^{+460}$  ms. We assume the  $\alpha$ 2 decay of group B represents a transition into an excited level of  $^{192}\text{Bi}$  not observed previously (see Fig. 7). Our assumption was confirmed by the observation of a weak  $\alpha$  transition from  $^{196}\text{At}$  with  $E_{\alpha} = 6742$  keV in a recent experiment at ISOLDE [37]. The half-life for  $^{196}\text{At}$  obtained from events of both groups, A and B, is 350(90) ms. Relative intensities of 96(2)% for the stronger line (group A) and 4(2)% for the weaker line (group B) were extracted from our data. From the difference of  $Q_{\alpha}$  values for both transitions we estimate the energy of the level populated in  $^{192}\text{Bi}$  by the 6732-keV transition as 320(10) keV. One  $\alpha$ 2 particle from group B came in coincidence with a  $\gamma$  ray at 76.5(6) keV. This energy agrees with the energy of  $K_{\alpha 1}$  x-rays of bismuth ( $E_{K_{\alpha 1}} = 77.107$  keV [13]). In addition, we observed one ER- $\alpha$ 1- $\alpha$ 2 correlation attributed to  $^{200}\text{Fr}$ - $^{196}\text{At}$  in the reaction with the  $^{149}\text{Sm}$  target. Both  $\alpha$  particles were fully stopped in the PSSD and the event is seen in Fig. 9(a).

In the reaction  $^{56}\text{Fe} + ^{147}\text{Sm}$  at  $E_{\text{beam}} = 263$  MeV one high-energy event was detected 67 ms after the ER implantation in the same position of the PSSD as the ER. The event was registered in the pause between beam pulses with signals from both PSSD and BOX detectors. The measured energy (not corrected for the pulse-height defect) of the event was

136(30) MeV (129 MeV in the PSSD and 7 MeV in the BOX system). We note that the energy calibration was performed using  $\alpha$  lines and was just extrapolated to higher energies from  $\alpha$ -decay energy region. Since no spontaneous-fission branch is known in any of the produced isotopes, we consider the observed event to be a candidate for  $\beta$ -delayed fission ( $\beta$ DF). The probability for the detection of the ER-fission correlation randomly is  $10^{-3}$ . Considering only fission events in the beam pauses, the 136(30)-MeV event was the only one between 50 and 250 MeV observed during the  $^{147}\text{Sm}$  irradiation of roughly 70 hours. In the comparably long measurement with the  $^{149}\text{Sm}$  target, no event was registered between 50 and 250 MeV in the pauses. The process of  $\beta$ DF was identified at SHIP recently in several other neutron-deficient isotopes above  $Z = 82$ , namely  $^{192,194}\text{At}$  [39] and  $^{186,188}\text{Bi}$  [40].

The ER-fission correlation was detected at a beam energy close to the expected maximum of the  $^{200}\text{Fr}$  excitation function. The half-life of the fission event ( $T_{1/2} = 47_{-20}^{+220}$  ms) is in excellent agreement with the 46(4)-ms half-life of  $^{200}\text{Fr}$ . Besides  $^{200}\text{Fr}$ , from the half-life point of view, the only other candidate for the observed fission is  $^{201}\text{Fr}$  ( $T_{1/2} = 64(3)$  ms) considering all nuclides produced in the reaction. However, we exclude  $^{201}\text{Fr}$  for two reasons: firstly,  $\beta$ DF of odd-even nuclei is suppressed compared to odd-odd nuclei [3]; and secondly, we did not register any fission event in the measurement with the  $^{149}\text{Sm}$  target, where about six times more  $^{201}\text{Fr}$  decay chains were collected compared to the measurement with the  $^{147}\text{Sm}$  target (see Sec. III E). Therefore we consider  $\beta$ DF of  $^{200}\text{Fr}$  to be the most probable source for the observed fission event. Recently,  $\beta$ DF events attributed to  $^{200}\text{Fr}$  were observed at ISOLDE as well [41].

Figure 8(a) shows a part of the  $\gamma$ -ray spectrum detected in the clover detector. The  $\gamma$  rays from panel (a) detected within a 5- $\mu$ s coincidence time with ERs implanted into the PSSD are shown in Fig. 8(b). Panel (c) shows  $\gamma$  rays from (b) followed by the  $\alpha$  decay of  $^{200}\text{Fr}$ . Insets in each panel show broader energy range for corresponding spectra. Pb x rays in panel (b) along with the intensive  $\gamma$  lines in the inset of panel (b) arise from the 11- $\mu$ s isomer in  $^{190}\text{Pb}$  produced in reactions with target contaminations. Because the most intensive lines in panels (a) and (b) (e.g., the 511-keV peak and  $\gamma$ -ray lines from the 11- $\mu$ s isomer in  $^{190}\text{Pb}$ ) are not present in panel (c), we assume that the lines in panel (c) are not random, but may arise from the decay of a short-lived isomeric state in  $^{200}\text{Fr}$ . The energies of  $\gamma$  lines at 83.8 (2 counts) and 86.6 keV (1 count) agree with  $K_{\alpha 2}$  and  $K_{\alpha 1}$  x rays of francium, respectively. Reference values are  $E_{K_{\alpha 2}} = 83.231$  keV,  $E_{K_{\alpha 1}} = 86.105$  keV [13]. Three other  $\gamma$  lines were registered at energies 75.5 (3 counts), 77.1 (4 counts) and 100.3 keV (2 counts) [see Fig. 8(c)]. All these energies are below the  $K$ -shell atomic-electron binding energy of francium (101.13 keV [13]). However, since we also observed  $K$  x rays, the excitation energy of the isomer must be higher than 101.13 keV (see Fig. 7). The half-life of this isomer is  $0.6_{-0.2}^{+0.5}$   $\mu$ s.

## 2. Discussion

Our measurement confirms the known  $\alpha$ -decay properties of  $^{200}\text{Fr}$  from previous studies (see Table III) by the detection of the 7470(5)-keV  $\alpha$  decay connecting the  $3^+$  states in  $^{200}\text{Fr}$  and

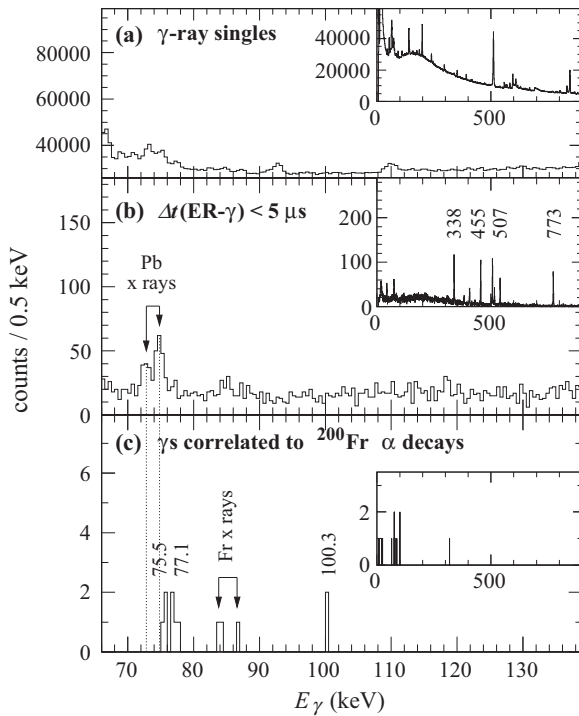


FIG. 8. (a) A part of the  $\gamma$ -ray spectrum detected in the germanium clover detector in the reaction  $^{56}\text{Fe} + ^{147}\text{Sm}$  at  $E_{\text{beam}} = 260$  and 263 MeV. (b) Gamma rays from (a) within a  $5\text{-}\mu\text{s}$  coincidence time with ERs implanted into the PSSD. (c) Gamma rays from (b) correlated with  $\alpha$  decays of  $^{200}\text{Fr}$ . Insets in each panel show unzoomed spectra.

$^{196}\text{At}$ . We observed a new  $\alpha$  line for the daughter nucleus  $^{196}\text{At}$  at 6732(8) keV populating a 320(10)-keV level in  $^{192}\text{Bi}$  (see the decay scheme in Fig. 7). The reduced  $\alpha$ -decay width for this transition is 17(9) keV using the measured relative intensity of

4% for this  $\alpha$  line. This decay is unhindered compared to the transitions connecting ground states with the same spins and parities between  $^{200}\text{At}$  and  $^{196}\text{Bi}$  with  $\delta_{\alpha}^2 = 18(2)$  keV [42] and between  $^{202}\text{At}$  and  $^{198}\text{Bi}$  with  $\delta_{\alpha}^2 = 12(2)$  keV [42]. Compared to the  $\alpha$  transitions connecting ground states with the same spins and parities of  $^{196,198}\text{At}$  and  $^{192,194}\text{Bi}$  with reduced widths of 29(8) and 39(5) keV [this work], respectively, the 6732(8)-keV decay is hindered up to about a factor of 2.

Besides the  $\alpha$ -decay mode of  $^{200}\text{Fr}$ , we also registered one  $\beta$ -delayed fission event attributed to this isotope. Due to the production of  $^{200}\text{Rn}$  in the  $2pn$  evaporation channel of the reaction  $^{56}\text{Fe} + ^{147}\text{Sm}$ , we could not estimate the  $\beta$  branch of  $^{200}\text{Fr}$  directly from our data. Based on the calculated partial  $\beta^+$ /EC-decay half-lives, the  $\beta$  branch can be estimated as about 1% according to Ref. [43], less than 2% according to Ref. [44], and about 4% according to Ref. [45]. From the experimental data measured at ISOLDE at CERN the  $\beta$  branch of less than 2.5% was estimated for  $^{200}\text{Fr}$  [41], which is close to theoretical predictions. Based on the ratio of detected  $\alpha$  decays of  $^{200}\text{Fr}$  and one event attributed to  $\beta$ -delayed fission of  $^{200}\text{Fr}$ , which is  $460_{-140}^{+1060}$ , and the estimated  $\beta$  branch of  $^{200}\text{Fr}$  of less than 2.5%, we determine the probability of  $\beta$ -delayed fission to be more than 1.4%.

## E. Isotope $^{201}\text{Fr}$

### 1. Experimental results

Two  $\alpha$ -decaying states in  $^{201}\text{Fr}$  were reported in Ref. [7]. The isotope was produced in the reactions  $^{63}\text{Cu} + ^{141}\text{Pr}$  at  $E_{\text{beam}} = (278\text{--}288)$  MeV and  $^{36}\text{Ar} + ^{170}\text{Yb}$  at  $E_{\text{beam}} = (180\text{--}185)$  MeV at RITU at JYFL. The stronger activity was assigned to the known decay of the  $9/2^-$  ground state. The weaker one comprising three correlation chains was assigned to the decay of the intruder  $1/2^+$  state. This assignment was based on the correlations with the known  $\alpha$  decay of the  $1/2^+$  state in the daughter nucleus  $^{197}\text{At}$ .

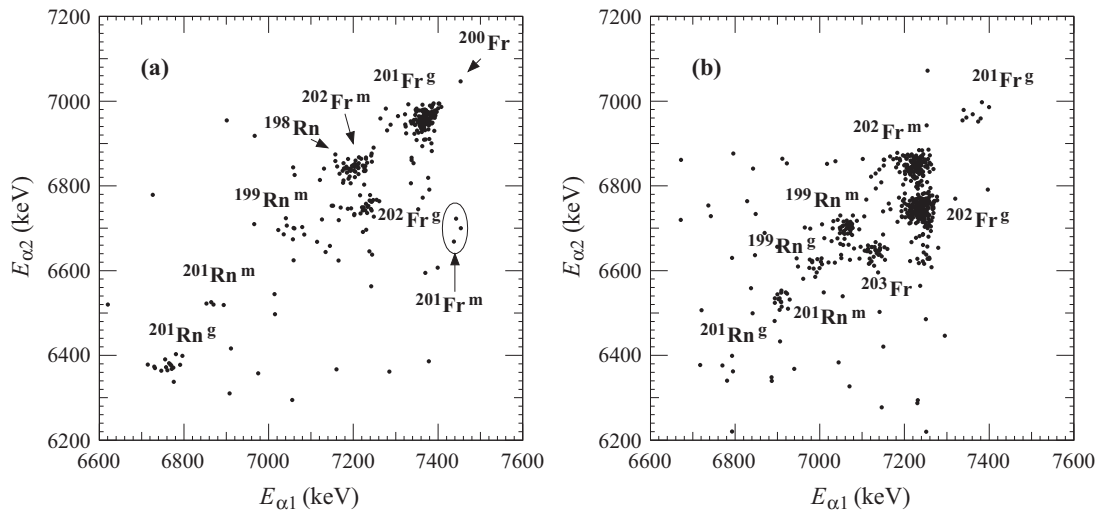


FIG. 9. Parent-daughter  $\alpha 1$ - $\alpha 2$  correlation energy spectra measured in the PSSD in anticoincidence with the TOF detectors in the reaction  $^{56}\text{Fe} + ^{149}\text{Sm}$ . The spectrum in panel (a) was measured at  $E_{\text{beam}} = 275$  MeV and the correlation search times were optimized for  $^{201}\text{Fr}^m$ :  $\Delta t(\text{ER}-\alpha 1) < 0.1$  s and  $\Delta t(\alpha 1-\alpha 2) < 12$  s. The spectrum in panel (b) was measured at  $E_{\text{beam}} = 256$  MeV and correlation search times were optimized for  $^{202}\text{Fr}$ :  $\Delta t(\text{ER}-\alpha 1) < 1.5$  s and  $\Delta t(\alpha 1-\alpha 2) < 10$  s.

TABLE IV. The  $\alpha$ -decay properties of  $^{201}\text{Fr}^{g,m}$  and its daughter  $^{197}\text{At}^{g,m}$ .

Isotope	$I^\pi$	$E_\alpha$ (keV)	$T_{1/2}$ (ms)	$\delta_\alpha^2$ (keV)	Ref.
$^{201}\text{Fr}$	$9/2^-$	7369(5)	64(3)	72(4)	this work
	$9/2^-$	7379(7)	67(3)	64(4)	[33]
	$9/2^-$	7369(8)	53(4)	87(8) <sup>a</sup>	[7]
	$9/2^-$	7361(7)	69 <sup>+16</sup> <sub>-11</sub>	71 <sup>+17</sup> <sub>-12</sub>	[32]
	$9/2^-$	7388(15)	48(15)	83(28) <sup>a</sup>	[46]
	$1/2^+$	7445(8)	8 <sup>+12</sup> <sub>-3</sub>	300 <sup>+500</sup> <sub>-100</sub>	this work
$^{197}\text{At}$	$1/2^+$	7454(8)	19 <sup>+19</sup> <sub>-6</sub>	130 <sup>+130</sup> <sub>-40</sub>	[7]
	$9/2^-$	6963(5)	354 <sup>+17</sup> <sub>-15</sub>	57 <sup>+4</sup> <sub>-3</sub>	this work
	$9/2^-$	6963(4)	390(16)	51(3)	[33]
	$9/2^-$	6959(6)	340(20)	61(5) <sup>a</sup>	[7]
	$9/2^-$	6960(5)	388(6)	53(2) <sup>a</sup>	[5]
	$9/2^-$	6956(5)	370 <sup>+90</sup> <sub>-60</sub>	57 <sup>+14</sup> <sub>-10</sub>	[32]
	$1/2^+$	6698(16)	2800 <sup>+3800</sup> <sub>-1000</sub>	70 <sup>+90</sup> <sub>-30</sub>	this work
	$1/2^+$	6706(9)	1100 <sup>+1100</sup> <sub>-400</sub>	160 <sup>+160</sup> <sub>-60</sub>	[7]
$1/2^+$	6707(5)	2000(200)	87(10) <sup>a</sup>	[5]	
$1/2^+$	6707	3700(2500)	47(32) <sup>a</sup>	[47]	

<sup>a</sup>See footnote in Table I.

We collected the main part of the data for  $^{201}\text{Fr}$  at  $E_{\text{beam}} = 275$  MeV in front of the  $^{149}\text{Sm}$  target, corresponding to a compound nucleus excitation energy of 53 MeV. A two-dimensional plot of correlated  $\alpha$ -decay parent-daughter ( $\alpha 1$ - $\alpha 2$ ) events is shown in Fig. 9(a). The dominant transition observed in our data connecting  $9/2^-$  ground states of  $^{201}\text{Fr}$  and  $^{197}\text{At}$  has decay properties consistent with reference values (see Table IV). The weak group of three events with  $E_{\alpha 1} = 7445(8)$  keV,  $T_{1/2} = 8_{-3}^{+12}$  ms for the parent  $\alpha 1$  decay, and  $E_{\alpha 2} = 6698(16)$  keV,  $T_{1/2} = 2.8_{-1.0}^{+3.8}$  s for the daughter  $\alpha 2$  decay was attributed to the decay of the intruder  $1/2^+$  state in  $^{201}\text{Fr}$ , which confirms the observation of this isomer in Ref. [7]. From the  $Q_\alpha$  values of ground- and isomeric-state decays and from the known excitation energy of the  $1/2^+$  level in  $^{197}\text{At}$ , we estimate the excitation energy of the  $1/2^+$  state in  $^{201}\text{Fr}$  to be 130(14) keV. This is in agreement with the value of 146 keV quoted in Ref. [7]. The isomeric ratio calculated from our data is 0.02(1). The cross section for the production of  $^{201}\text{Fr}$  of 4.0(4) nb was measured at  $E_{\text{beam}} = 275$  MeV corresponding to the expected maximum of the  $^{201}\text{Fr}$  excitation function. We did not observe any  $^{201}\text{Fr}^m - ^{197}\text{At}^g$  correlations.

Figure 10(a) shows a part of the  $\gamma$ -ray spectrum detected in the germanium clover detector without any selection conditions applied. Panel (b) shows  $\gamma$  rays detected within a 5- $\mu\text{s}$  coincidence time with ERs implanted into the PSSD. Panel (c) was obtained applying the condition of detecting an  $\alpha$  decay from  $^{201}\text{Fr}$  after ER- $\gamma$  coincidences from panel (b). Insets in panels (a), (b), (c) show a broader energy range for the corresponding spectra. As the most intense peaks from panels (a) and (b) are not reproduced in panel (c), we assume that the peak at 85.7 keV (7 counts) in this panel is not random, but may originate from the decay of a short-lived isomer in

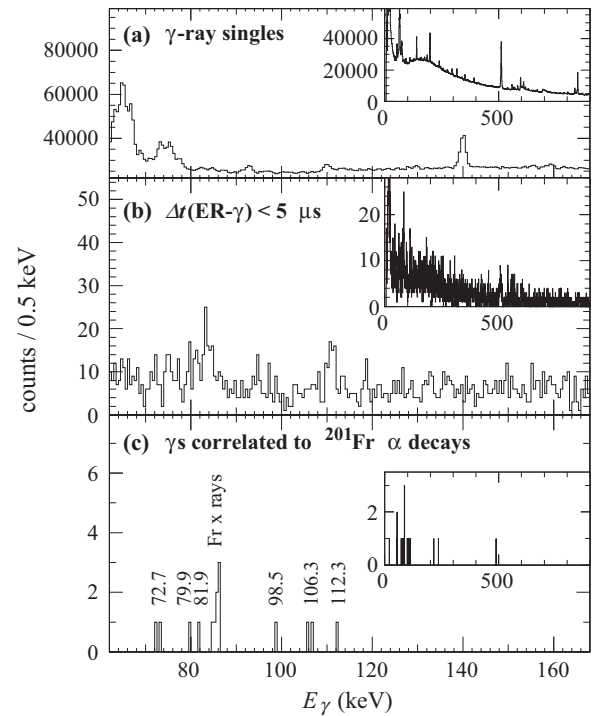


FIG. 10. (a) A part of the  $\gamma$ -ray spectrum detected in the germanium clover detector in the reaction  $^{56}\text{Fe} + ^{149}\text{Sm}$  at  $E_{\text{beam}} = 275$  MeV. (b) Gamma rays from (a) within a 5- $\mu\text{s}$  coincidence time with ERs implanted into the PSSD. (c) Gamma rays from (b) correlated with  $\alpha$  decays of  $^{201}\text{Fr}$ . Insets in each panel show unzoned spectra.

$^{201}\text{Fr}$ . The energy of the peak corresponds to the energy of  $K_{\alpha 1}$  x rays of francium, which is 86.105 keV [13]. As the intensity ratio  $I_{K_{\alpha 2}}/I_{K_{\alpha 1}} = 0.61(2)$  [13], one should expect the detection of about four  $K_{\alpha 2}$  x rays. Since none were observed, we note that possibly at least some of the events at 85.7 keV may not be x rays, but  $\gamma$  rays. Other weak  $\gamma$ -ray lines were registered at 72.7 and 106.3 keV (2 counts for each line). The half-life of the isomer is  $0.7_{-0.2}^{+0.5}$   $\mu\text{s}$ .

## 2. Discussion

Our measurement confirms the presence of the  $\alpha$ -decaying isomeric  $1/2^+$  level in  $^{201}\text{Fr}$  reported in Ref. [7]. Besides this level, we observed a short-lived activity, which may be assigned to another isomeric level in  $^{201}\text{Fr}$ . This assignment is based on the detection of francium  $K_{\alpha 1}$  x rays (7 counts) and two weak lines in the  $\gamma$ -ray spectrum at 72.7 and 106.3 keV (2 counts for each line) within a 5- $\mu\text{s}$  coincidence time with ERs of  $^{201}\text{Fr}$ . We note that the detection setup was not optimized for the detection of  $L$  x rays. The source of  $K_{\alpha 1}$  x rays must be a transition with an energy higher than the  $K$ -shell binding energy of francium (101.13 keV [13]). We can consider two possibilities: observed  $K_{\alpha 1}$  x rays come from the internal conversion of (a) the 106.3-keV internal transition, or (b) an unobserved internal transition with an energy larger than the  $K$ -shell binding energy (101.13 keV). The  $K$ -shell internal conversion coefficient ( $\alpha_K$ ) from experimental data is roughly 4 for variant (a) and more than 7 for variant (b).

TABLE V. Comparison of total ( $\alpha_{\text{tot}}$ ) and K-shell ( $\alpha_K$ ) internal conversion coefficients from Ref. [49] and single-particle half-lives ( $T_{1/2,SP}$ ) according to Weisskopf [48] for the 106.3-keV internal transition of different multiplicities in the nuclide  $^{201}\text{Fr}$ .

Multipolarity	$\alpha_{\text{tot}}$	$\alpha_K$	$T_{1/2,SP}$
$E1$	0.406(6)	0.315(5)	0.1 ps
$E2$	6.91(10)	0.311(5)	80 ns
$E3$	167.5(24)	0.1302(19)	20 ms
$M1$	12.00(17)	9.64(14)	1 ps
$M2$	89.2(13)	54.0(8)	0.8 $\mu\text{s}$
$M3$	645(9)	72.8(11)	0.6 s

For both variants we exclude an electric character of the internal transition producing  $K_{\alpha 1}$  x rays because the expected  $\alpha_K$  values are too low. [See Table V showing expected  $\alpha_K$  values for the 106.3-keV transition corresponding to variant (a). For transitions of higher energies the  $\alpha_K$  values would be even lower excluding variant (b) as well.] In contrast,  $M2$  and higher magnetic multiplicities have too high  $\alpha_K$  values for case (a), but for case (b) all multiplicities for magnetic transitions would be compatible with experimental  $\alpha_K$ .

Considering the Weisskopf estimates for single-particle half-lives ( $T_{1/2,SP}$ ) according to Ref. [48], we exclude  $E1$ ,  $E2$ , and  $M1$  characters as candidates for the transition producing observed  $K_{\alpha 1}$  x rays, because their  $T_{1/2,SP}$  is much shorter than the measured value of  $0.7_{-0.2}^{+0.5}$   $\mu\text{s}$  (see Table V). On the other hand,  $T_{1/2,SP}$  for transitions of  $E3$  and  $M3$  characters (and higher multiplicities) is significantly longer than the measured value. We note that there are several known cases of isomers decaying by  $E1$  transitions with relatively long half-lives, but as we also excluded electric characters based on  $\alpha_K$  values, it does not influence our conclusions. Therefore, considering the measured half-life,  $M2$  is the most likely multipolarity for the transition producing the observed  $K_{\alpha 1}$  x rays.

To conclude, we assume the observed  $K_{\alpha 1}$  x rays arise from an internal transition of  $M2$  character, for which  $\gamma$ -ray events were not observed due to a high  $\alpha_K$  value. Assuming that the isomer decays directly by this transition to the  $9/2^-$  ground state, we tentatively assign a spin and parity of  $13/2^+$  to this isomeric state (see the decay scheme in Fig. 11). The excitation energy of the isomer must be higher than the  $K$ -shell atomic-electron binding energy of francium, which is 101.13 keV [13]. The upper limit for the excitation energy can be deduced to be roughly 300 keV from the trend of decreasing  $\alpha_K$  as a function of energy for an  $M2$  transition.

We note that an isomeric state with spin and parity  $13/2^+$  decaying through an  $M2$  internal transition to the  $9/2^-$  ground state was observed in  $^{203}\text{Fr}$  at  $E^* = 426$  keV with  $T_{1/2} = 0.37(5)$   $\mu\text{s}$  [8] and in  $^{205}\text{Fr}$  at  $E^* = 544$  keV with  $T_{1/2} = 80(20)$  ns [9]. The estimated energy range for the excitation energy of the isomer in  $^{201}\text{Fr}$ ,  $\sim(101-300)$  keV, confirms the trend of the decreasing excitation energy of the  $13/2^+$  isomer with decreasing  $N$  in odd- $A$  francium isotopes (see Fig. 12). This level is also present in odd- $A$  astatine and

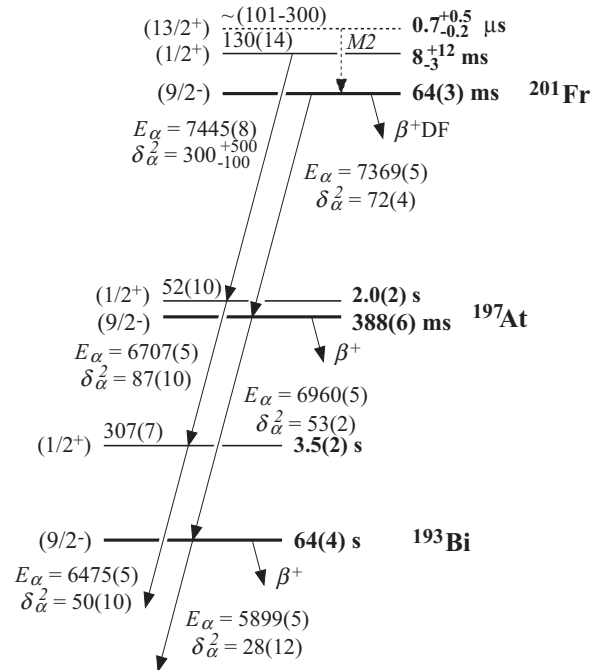


FIG. 11. Decay scheme for  $^{201}\text{Fr}$ . Values for  $^{201}\text{Fr}$  are from this work, for  $^{197}\text{At}$  from Refs. [5,47] and for  $^{193}\text{Bi}$  from Ref. [4] and references therein. Alpha-decay energies, reduced widths and energies of excited levels are in keV.

bismuth isotopes and its energy decreases with decreasing neutron numbers as well.

The  $13/2^+$  and  $1/2^+$  states appear very close in energy in the most neutron-deficient francium isotopes, while in astatine

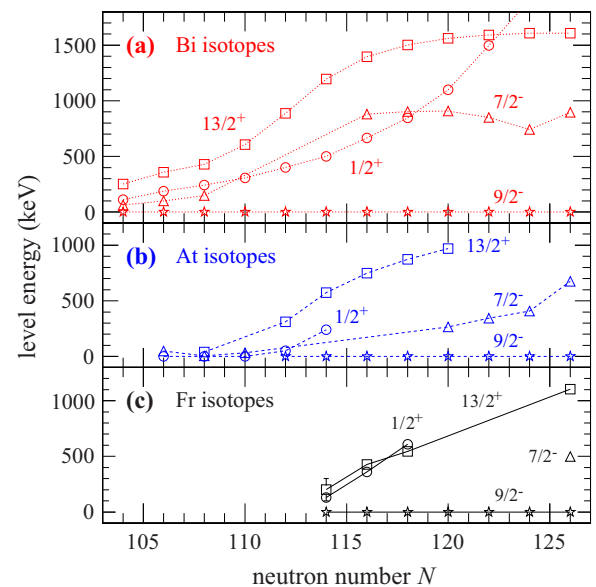


FIG. 12. (Color online) Single-particle level systematics for odd- $A$  (a) bismuth ( $Z = 83$ ), (b) astatine ( $Z = 85$ ), and (c) francium ( $Z = 87$ ) isotopes. The error bar for the  $13/2^+$  state in  $^{201}\text{Fr}$  ( $N = 114$ ) corresponds to the possible energy interval for this state; the exact value is not known. Reference values are taken from Refs. [8,9,26].

and bismuth isotopes clear differences in excitation energy between these states exist (see Fig. 12). It might mean that in the lightest francium isotopes the  $13/2^+$  state becomes the ground state, in contrast to the lightest astatine isotopes, where the intruder  $1/2^+$  state becomes the ground state. Besides the  $13/2^+$  and  $1/2^+$  levels, the  $7/2^-$  level has decreasing energy with decreasing  $N$  in astatine and bismuth isotopes as well. In recent measurements at SHIP we observed decays of this level ( $7/2^-$ ) in  $^{199}\text{Fr}$  ( $N = 112$ ) and  $^{197}\text{Fr}$  ( $N = 110$ ), but we could not establish its excitation energy [50]. We also reported a possible observation of the  $1/2^+$  level 47(7) keV below the  $7/2^-$  level in  $^{199}\text{Fr}$ . Besides our study, another study of  $^{199}\text{Fr}$  was performed [34], where three levels were suggested: the ground  $1/2^+$  state, the  $7/2^-$  state at 56 keV and the  $13/2^+$  state at  $\leq 300$  keV. As the results from both experiments are not unambiguous, we did not place these levels in  $^{199}\text{Fr}$  in Fig. 12. To investigate the energy levels in the most neutron-deficient francium isotopes in more detail, measurements with higher statistics must be performed.

Considering the tentative excitation energy range of (101–300) keV, the transition strength for the  $M2$  multipolarity is (0.2–1.1) W.u. This is comparable to B(M2) values for neighboring odd- $A$  francium isotopes: 0.10(2) W.u. for  $^{203}\text{Fr}$  [8], 0.17(4) W.u. for  $^{205}\text{Fr}$  [9]; and astatine isotopes: 0.09(1) for  $^{197}\text{At}$  [51], 0.16(5) W.u. for  $^{199}\text{At}$  [52], 0.15(1) for  $^{201}\text{At}$  [53].

## F. Isotope $^{202}\text{Fr}$

### 1. Experimental results and discussion

The presence of two  $\alpha$ -decaying states in  $^{202}\text{Fr}$  was mentioned in Ref. [42] for the first time. In that study the isotope  $^{202}\text{Fr}$  was produced at Leuven Isotope Separator On-Line (LISOL) facility (Louvain-la-Neuve, Belgium). The states with spins and parities  $3^+$  (ground state) and  $10^-$  (isomeric state) were assumed to decay to corresponding levels in  $^{198}\text{At}$ . Although two states were reported, only one  $\alpha$  line was observed, which was interpreted as a line doublet. Also only a common half-life for both states was given. In later experiments at RITU (JYFL) these two  $\alpha$  lines were confirmed and disentangled using the  $\alpha$ - $\alpha$  correlation technique [7,32] (see Table VI).

In our study we collected the data for  $^{202}\text{Fr}$  at several beam energies in the range of (244–275) MeV in front of the  $^{149}\text{Sm}$  target. The majority of  $^{202}\text{Fr}$  nuclei were produced at  $E_{\text{beam}} = 256$  MeV corresponding to a 39-MeV excitation energy of compound nuclei. A two-dimensional plot of parent-daughter ( $\alpha 1$ - $\alpha 2$ ) correlations measured at this energy is shown in Fig. 9(b). In total around 500  $\alpha 1$ - $\alpha 2$  pairs of  $^{202}\text{Fr}$ - $^{198}\text{At}$  were registered. We observed  $\alpha$  decays of two states in  $^{202}\text{Fr}$  correlated with the  $\alpha$  decays of two corresponding states in the daughter nuclide  $^{198}\text{At}$ . The isomeric ratio is 0.6(1) from our data. For the sum of both states, the maximum cross section of 25(2) nb was measured at  $E_{\text{beam}} = 256$  MeV corresponding to the maximum of the  $^{202}\text{Fr}$  excitation function.

## IV. SUMMARY

We investigated the  $\alpha$ -decay properties of neutron-deficient isotopes  $^{201-203}\text{Ra}$  and  $^{200-202}\text{Fr}$  produced in the

TABLE VI. The  $\alpha$ -decay properties of  $^{202}\text{Fr}^{g,m}$  and its daughter  $^{198}\text{At}^{g,m}$ .

Isotope	$I^\pi$	$E_\alpha$ (keV)	$T_{1/2}$ (s)	$\delta_\alpha^2$ (keV)	Ref.	
$^{202}\text{Fr}$	$3^+$	7238(5)	0.372(12)	33(2)	this work	
	$3^+$	7241(8)	0.30(5)	40(7) <sup>a</sup>	[7]	
	$3^+$	7243(6)	$0.23_{-0.04}^{+0.08}$	$52_{-9}^{+18a}$	[32]	
	$3^+$	7237(8)	0.34(4)	$\leq 53$	[42]	
	$10^-$	7226(5)	0.286(13)	48(3)	this work	
	$10^-$	7235(8)	0.29(5)	44(8) <sup>a</sup>	[7]	
	$10^-$	7242(6)	$0.23_{-0.5}^{+0.14}$	$52_{-12}^{+32a}$	[32]	
	$10^-$	7237(8)	0.34(4)	$\leq 53$	[42]	
	$^{198}\text{At}$	$3^+$	6747(5)	3.0(1)	39(2)	this work
		$3^+$	6748(6)	3.8(4)	27(5) <sup>a</sup>	[7]
$3^+$		6753(4)	$4.6_{-1.0}^{+1.8}$	$22_5^{+9a}$	[32]	
$3^+$		6755(4)	4.2(3)	26 – 37	[42]	
$10^-$		6849(5)	1.24(6)	39(3)	this work	
$10^-$		6850(6)	1.04(15)	39(10) <sup>a</sup>	[7]	
$10^-$		6855(4)	$1.3_{-0.3}^{+0.8}$	[32]		
$10^-$		6856(4)	1.0(2)	37 – 73	[42]	

<sup>a</sup>See footnote in Table I.

fusion-evaporation reaction  $^{56}\text{Fe} + ^{147,149}\text{Sm}$ . A new  $\alpha$ -decaying state in  $^{201}\text{Ra}$  was observed yielding  $E_\alpha = 7842(12)$  keV and  $T_{1/2} = 8_{-4}^{+40}$  ms. Based on the unhindered nature of this decay we assume that it originates from a  $3/2^-$  state and populates a state with the same spin and parity in  $^{197}\text{Rn}$ . For the heavier radium isotope  $^{202}\text{Ra}$  we significantly improved the  $\alpha$ -decay data compared to previous studies and obtained  $E_\alpha = 7722(7)$  keV and  $T_{1/2} = 3.8_{-0.8}^{+1.3}$  ms. The reduced  $\alpha$ -decay width ( $\delta_\alpha^2$ ) of  $210_{-50}^{+70}$  keV for this transition shows a trend of increasing  $\delta_\alpha^2$  for radium isotopes at decreasing neutron numbers.

A new weak  $\alpha$  line at 6732(8) keV was observed in  $^{196}\text{At}$ , the  $\alpha$ -decay daughter of  $^{200}\text{Fr}$ . Gamma rays registered within a 5- $\mu\text{s}$  coincidence time after implantation of  $^{200}\text{Fr}$  and  $^{201}\text{Fr}$  nuclei were registered. They indicate the existence of short-lived isomeric states in each of these isotopes with half-lives of  $0.6_{-0.2}^{+0.5}$   $\mu\text{s}$  ( $^{200}\text{Fr}$ ) and  $0.7_{-0.2}^{+0.5}$   $\mu\text{s}$  ( $^{201}\text{Fr}$ ). A spin and parity of  $13/2^+$  were tentatively assigned to this short-lived state in  $^{201}\text{Fr}$ . In the isotope  $^{200}\text{Fr}$  a branch of  $\beta$ -delayed fission ( $\beta\text{DF}$ ) was identified based on one fission event. The estimated lower limit for the  $\beta\text{DF}$  probability is 1.4%. In addition, we remeasured and confirmed previous results for  $^{203}\text{Ra}$  and  $^{202}\text{Fr}$ .

## ACKNOWLEDGMENTS

We thank the UNILAC staff for providing the stable and high intensity  $^{56}\text{Fe}$  beam. This work was supported by FWO-Vlaanderen (Belgium), GOA/2004/03 (BOF-KU Leuven), IUAP – Belgian State Belgian Science Policy (BriX network P7/12), the European Community FP7 Capacities, Contract ENSAR No. 227867, the UK Science and Technology Facilities Council (STFC), the Slovak Research and

Development Agency (Contracts No. APVV-0105-10 and No. APVV-0177-11), the Slovak grant agency VEGA (Contract No. 1/0576/13), a Comenius University grant (Con-

tract No. UK/28/2013), the Reimei Foundation of Advanced Science Research Center (ASRC, JAEA), and the DAIWA Anglo-Japanese Foundation.

- [1] K. Heyde and J. L. Wood, *Rev. Mod. Phys.* **83**, 1467 (2011).
- [2] H. L. Hall and D. C. Hoffman, *Annu. Rev. Nucl. Part. Sci.* **42**, 147 (1992).
- [3] A. N. Andreyev, M. Huyse, and P. Van Duppen, *Rev. Mod. Phys.* **85**, 1541 (2013).
- [4] E. Coenen, K. Deneffe, M. Huyse, P. Van Duppen, and J. L. Wood, *Phys. Rev. Lett.* **54**, 1783 (1985).
- [5] M. B. Smith, R. Chapman, J. F. C. Cocks, O. Dorvaux, K. Helariutta, P. M. Jones, R. Julin, S. Juutinen, H. Kankaanpää, H. Kettunen, P. Kuusiniemi, Y. Le Coz, M. Leino, D. J. Middleton, M. Muikku, P. Nieminen, P. Rakhila, A. Savelius, and K.-M. Spohr, *Eur. Phys. J. A* **5**, 43 (1999).
- [6] A. N. Andreyev, D. Ackermann, F. P. Heßberger, K. Heyde, S. Hofmann, M. Huyse, D. Karlgren, I. Kojouharov, B. Kindler, B. Lommel, G. Münzenberg, R. D. Page, K. Van de Vel, P. Van Duppen, W. B. Walters, and R. Wyss, *Phys. Rev. C* **69**, 054308 (2004).
- [7] J. Uusitalo, M. Leino, T. Enqvist, K. Eskola, T. Grahn, P. T. Greenlees, P. Jones, R. Julin, S. Juutinen, A. Keenan, H. Kettunen, H. Koivisto, P. Kuusiniemi, A.-P. Leppänen, P. Nieminen, J. Pakarinen, P. Rakhila, and C. Scholey, *Phys. Rev. C* **71**, 024306 (2005).
- [8] U. Jakobsson, S. Juutinen, J. Uusitalo, M. Leino, K. Auranen, T. Enqvist, P. T. Greenlees, K. Hauschild, P. Jones, R. Julin, S. Ketelhut, P. Kuusiniemi, M. Nyman, P. Peura, P. Rakhila, P. Ruotsalainen, J. Sarén, C. Scholey, and J. Sorri, *Phys. Rev. C* **87**, 054320 (2013).
- [9] U. Jakobsson, J. Uusitalo, S. Juutinen, M. Leino, T. Enqvist, P. T. Greenlees, K. Hauschild, P. Jones, R. Julin, S. Ketelhut, P. Kuusiniemi, M. Nyman, P. Peura, P. Rakhila, P. Ruotsalainen, J. Sarén, C. Scholey, and J. Sorri, *Phys. Rev. C* **85**, 014309 (2012).
- [10] K. Helariutta, J. F. C. Cocks, T. Enqvist, P. T. Greenlees, P. Jones, R. Julin, S. Juutinen, P. Jämsen, H. Kankaanpää, H. Kettunen, P. Kuusiniemi, M. Leino, M. Muikku, M. Piiparinen, P. Rakhila, A. Savelius, W. H. Trzaska, S. Törmänen, J. Uusitalo, R. G. Allatt, P. A. Butler, R. D. Page, and M. Kapusta, *Eur. Phys. J. A* **6**, 289 (1999).
- [11] D. J. Dobson, S. J. Freeman, P. T. Greenlees, A. N. Qadir, S. Juutinen, J. L. Durell, T. Enqvist, P. Jones, R. Julin, A. Keenan, H. Kettunen, P. Kuusiniemi, M. Leino, P. Nieminen, P. Rakhila, S. D. Robinson, J. Uusitalo, and B. J. Varley, *Phys. Rev. C* **66**, 064321 (2002).
- [12] G. Münzenberg, W. Faust, S. Hofmann, P. Armbruster, K. Güttnert, and H. Ewald, *Nucl. Instrum. Methods* **161**, 65 (1979).
- [13] R. B. Firestone and L. P. Ekström, database version 2.1, 2004, <http://ie.lbl.gov/toi/perchart.htm>.
- [14] A. N. Andreyev, D. Ackermann, F. P. Heßberger, S. Hofmann, M. Huyse, G. Münzenberg, R. D. Page, K. Van de Vel, and P. Van Duppen, *Nucl. Instrum. Methods A* **533**, 409 (2004).
- [15] Š. Šáro, R. Janik, S. Hofmann, H. Folger, F. P. Heßberger, V. Ninov, H. J. Schött, A. P. Kabachenko, A. G. Popeko, and A. V. Yeremin, *Nucl. Instrum. Methods A* **381**, 520 (1996).
- [16] F. P. Heßberger, S. Antalic, B. Sulignano, D. Ackermann, S. Heinz, S. Hofmann, B. Kindler, J. Khuyagbaatar, I. Kojouharov, P. Kuusiniemi, M. Leino, B. Lommel, R. Mann, K. Nishio, A. G. Popeko, Š. Šáro, B. Streicher, J. Uusitalo, M. Venhard, and A. V. Yeremin, *Eur. Phys. J. A* **43**, 55 (2010).
- [17] S. Hofmann, W. Faust, G. Münzenberg, W. Reisdorf, P. Armbruster, K. Güttnert, and H. Ewald, *Z. Phys. A* **291**, 53 (1979).
- [18] M. Leino, J. Uusitalo, R. G. Allatt, P. Armbruster, T. Enqvist, K. Eskola, S. Hofmann, S. Hurskanen, A. Jokinen, V. Ninov, R. D. Page, and W. H. Trzaska, *Z. Phys. A* **355**, 157 (1996).
- [19] N. Bijmens, P. Decroock, S. Franchoo, M. Gaelens, M. Huyse, H.-Y. Hwang, I. Reusen, J. Szerypo, J. von Schwarzenberg, J. Wauters, J. G. Correia, A. Jokinen, P. Van Duppen, and The ISOLDE Collaboration, *Phys. Rev. Lett.* **75**, 4571 (1995).
- [20] J. Wauters, P. Dendooven, M. Huyse, G. Reusen, P. Van Duppen, P. Lievens, and the ISOLDE Collaboration, *Phys. Rev. C* **47**, 1447 (1993).
- [21] J. O. Rasmussen, *Phys. Rev.* **113**, 1593 (1959).
- [22] A. N. Andreyev, M. Huyse, P. Van Duppen, C. Qi, R. J. Liotta, S. Antalic, D. Ackermann, S. Franchoo, F. P. Heßberger, S. Hofmann, I. Kojouharov, B. Kindler, P. Kuusiniemi, S. R. Leshner, B. Lommel, R. Mann, K. Nishio, R. D. Page, B. Streicher, Š. Šáro, B. Sulignano, D. Wiseman, and R. A. Wyss, *Phys. Rev. Lett.* **110**, 242502 (2013).
- [23] J. A. Heredia, A. N. Andreyev, S. Antalic, S. Hofmann, D. Ackermann, V. F. Comas, S. Heinz, F. P. Heßberger, B. Kindler, J. Khuyagbaatar, B. Lommel, and R. Mann, *Eur. Phys. J. A* **46**, 337 (2010).
- [24] A. N. Andreyev, S. Antalic, M. Huyse, P. Van Duppen, D. Ackermann, L. Bianco, D. M. Cullen, I. G. Darby, S. Franchoo, S. Heinz, F. P. Heßberger, S. Hofmann, I. Kojouharov, B. Kindler, A.-P. Leppänen, B. Lommel, R. Mann, G. Münzenberg, J. Pakarinen, R. D. Page, J. J. Ressler, Š. Šáro, B. Streicher, B. Sulignano, J. Thomson, and R. Wyss, *Phys. Rev. C* **74**, 064303 (2006).
- [25] H. Kettunen, J. Uusitalo, M. Leino, P. Jones, K. Eskola, P. T. Greenlees, K. Helariutta, R. Julin, S. Juutinen, H. Kankaanpää, P. Kuusiniemi, M. Muikku, P. Nieminen, and P. Rakhila, *Phys. Rev. C* **63**, 044315 (2001).
- [26] Data extracted using the NNDC On-Line Data Service from the ENSDF database, file revised as of 2014-01-08. M. R. Bhat, Evaluated Nuclear Structure Data File (ENSDF), Nuclear Data for Science and Technology, [www.nndc.bnl.gov](http://www.nndc.bnl.gov).
- [27] T. Enqvist, P. Armbruster, K. Eskola, M. Leino, V. Ninov, W. H. Trzaska, and J. Uusitalo, *Z. Phys. A* **354**, 9 (1996).
- [28] K.-H. Schmidt, *Z. Phys. A* **316**, 19 (1984).
- [29] J. Sauvage, B. Rousseau, J. Genevey, S. Franchoo, A. N. Andreyev, N. Barré, A. Ben Braham, C. Bourgeois, J.-F. Clavelin, H. De Witte, D. V. Fedorov, V. N. Fedoseyev, L. M. Fraile, X. Grave, G. Huber, M. Huyse, P. Kilcher, U. Köster, P. Kunz, S. R. Leshner, B. A. Marsh, I. Mukha, J. Oms, M. G. Porquet, M. Seliverstov, I. Stefanescu, K. Van de Vel, P. Van Duppen, Y. M. Volkov, and A. Wojtasiewicz, *Eur. Phys. J. A* **49**, 109 (2013).
- [30] F. Calaprice, G. T. Ewan, R.-D. von Dincklage, B. Jonson, O. C. Jonsson, and H. L. Ravn, *Phys. Rev. C* **30**, 1671 (1984).
- [31] K. Morita, Y. H. Pu, J. Feng, M. G. Hies, K. O. Lee, A. Yoshida, S. C. Jeong, S. Kubono, T. Nomura, Y. Tagaya, M. Wada, M.

- Kurokawa, T. Motobayashi, H. Ogawa, T. Uchibori, K. Sueki, T. Ishizuka, K. Uchiyama, Y. Fujita, H. Miyatake, T. Shimoda, T. Shinozuka, H. Kudo, Y. Nagai, and S. A. Shin, *Z. Phys. A* **352**, 7 (1995).
- [32] T. Enqvist, K. Eskola, A. Jokinen, M. Leino, W. H. Trzaska, J. Uusitalo, V. Ninov, and P. Armbruster, *Z. Phys. A* **354**, 1 (1996).
- [33] H. De Witte, A. N. Andreyev, S. Dean, S. Franchoo, M. Huyse, O. Ivanov, U. Köster, W. Kurcewicz, J. Kurpeta, A. Plochocki, K. Van de Vel, J. Van de Walle, and P. Van Duppen, *Eur. Phys. J. A* **23**, 243 (2005).
- [34] J. Uusitalo, J. Sarén, S. Juutinen, M. Leino, S. Eeckhaudt, T. Grahn, P. T. Greenlees, U. Jakobsson, P. Jones, R. Julin, S. Ketelhut, A.-P. Leppänen, M. Nyman, J. Pakarinen, P. Rahkila, C. Scholey, A. Semchenkov, J. Sorri, A. Steer, and M. Venhart, *Phys. Rev. C* **87**, 064304 (2013).
- [35] M. B. Smith, R. Chapman, J. F. C. Cocks, K.-M. Spohr, O. Dorvaux, K. Helariutta, P. M. Jones, R. Julin, S. Juutinen, H. Kankaanpää, H. Kettunen, P. Kuusiniemi, Y. Le Coz, M. Leino, D. J. Middleton, M. Muikku, P. Nieminen, P. Rahkila, and A. Savelius, *J. Phys. G: Nucl. Part. Phys.* **26**, 787 (2000).
- [36] Y. H. Pu, K. Morita, M. G. Hies, K. O. Lee, A. Yoshida, T. Nomura, Y. Tagaya, T. Motobayashi, M. Kurokawa, H. Minemura, T. Uchibori, T. Ariga, K. Sueki, and S. A. Shin, *Z. Phys. A* **357**, 1 (1997).
- [37] V. Truesdale *et al.* (unpublished).
- [38] P. Van Duppen, P. Decrock, P. Dendooven, M. Huyse, G. Reusen, and J. Wauters, *Nucl. Phys. A* **529**, 268 (1991).
- [39] A. N. Andreyev, S. Antalic, D. Ackermann, L. Bianco, S. Franchoo, S. Heinz, F. P. Heßberger, S. Hofmann, M. Huyse, Z. Kalaninová, I. Kojouharov, B. Kindler, B. Lommel, R. Mann, K. Nishio, R. D. Page, J. J. Ressler, B. Streicher, Š. Šáro, B. Sulignano, and P. Van Duppen, *Phys. Rev. C* **87**, 014317 (2013).
- [40] J. F. W. Lane, A. N. Andreyev, S. Antalic, D. Ackermann, J. Gerl, F. P. Heßberger, S. Hofmann, M. Huyse, H. Kettunen, A. Kleinböhl, B. Kindler, I. Kojouharov, M. Leino, B. Lommel, G. Münzenberg, K. Nishio, R. D. Page, Š. Šáro, H. Schaffner, M. J. Taylor, and P. Van Duppen, *Phys. Rev. C* **87**, 014318 (2013).
- [41] L. Ghys *et al.* (unpublished).
- [42] M. Huyse, P. Decrock, P. Dendooven, G. Reusen, P. Van Duppen, and J. Wauters, *Phys. Rev. C* **46**, 1209 (1992).
- [43] K. Takahashi, M. Yamada, and T. Kondoh, *At. Data Nucl. Data Tables* **12**, 101 (1973).
- [44] M. Hirsch, A. Staudt, K. Muto, and H. V. Klapdor-Kleingrothaus, *At. Data Nucl. Data Tables* **53**, 165 (1993).
- [45] P. Möller, J. R. Nix, and K.-L. Kratz, *At. Data Nucl. Data Tables* **66**, 131 (1997).
- [46] G. T. Ewan, E. Hagberg, B. Jonson, S. Mattsson, and P. Tidemand-Petersson, *Z. Phys. A* **296**, 223 (1980).
- [47] E. Coenen, K. Deneffe, M. Huyse, and P. Van Duppen, *Z. Phys. A* **324**, 485 (1986).
- [48] V. F. Weisskopf, *Phys. Rev.* **83**, 1073 (1951).
- [49] T. Kibédi, T. W. Burrows, M. B. Trzhaskovskaya, P. M. Davidson, and C. W. N., Jr., *Nucl. Instrum. Methods A* **589**, 202 (2008), <http://bricc.anu.edu.au/>.
- [50] Z. Kalaninová, A. N. Andreyev, S. Antalic, F. P. Heßberger, D. Ackermann, B. Andel, M. C. Drummond, S. Hofmann, M. Huyse, B. Kindler, J. F. W. Lane, V. Liberati, B. Lommel, R. D. Page, E. Rapisarda, K. Sandhu, Š. Šáro, A. Thornthwaite, and P. Van Duppen, *Phys. Rev. C* **87**, 044335 (2013).
- [51] K. Andgren, U. Jakobsson, B. Cederwall, J. Uusitalo, T. Bäck, S. J. Freeman, P. T. Greenlees, B. Hadinia, A. Hugues, A. Johnson, P. M. Jones, D. T. Joss, S. Juutinen, R. Julin, S. Ketelhut, A. Khaplanov, M. Leino, M. Nyman, R. D. Page, P. Rahkila, M. Sandzelius, P. Sapple, J. Sarén, C. Scholey, J. Simpson, J. Sorri, J. Thomson, and R. Wyss, *Phys. Rev. C* **78**, 044328 (2008).
- [52] U. Jakobsson, J. Uusitalo, S. Juutinen, M. Leino, P. Nieminen, K. Andgren, B. Cederwall, P. T. Greenlees, B. Hadinia, P. Jones, R. Julin, S. Ketelhut, A. Khaplanov, M. Nyman, P. Peura, P. Rahkila, P. Ruotsalainen, M. Sandzelius, J. Sarén, C. Scholey, and J. Sorri, *Phys. Rev. C* **82**, 044302 (2010).
- [53] K. Dybdal, T. Chapuran, D. B. Fossan, W. F. Piel, Jr., D. Horn, and E. K. Warburton, *Phys. Rev. C* **28**, 1171 (1983).